Clinical Neurophysiology 184 (2026) 2111506

Contents lists available at ScienceDirect

Clinical Neurophysiology

journal homepage: www.elsevier.com/locate/clinph

Lacosamide modulates alpha-band network hubness: a quantitative EEG study in drug-Naïve focal epilepsy

Marco Sferruzzi [a], Lorenzo Ricci [a,b,*], Margherita A.G. Matarrese [c], Mario Tombini [a,d], Patrizia Pulitano [e], Francesca Izzi [f], Fabio Placidi [f], Biagio Sancetta [a], Vincenzo Di Lazzaro [a,d], Giovanni Assenza [a,d]

[a] Department of Medicine and Surgery, Research Unit of Neurology, Neurobiology, Neurophysiology, University Campus Bio-Medico di Roma, Rome, Italy
[b] Cumming School of Medicine, University of Calgary, Calgary, Canada
[c] Department of Engineering, Research Unit of Intelligent Health Technology, University Campus Bio-Medico di Roma, Rome, Italy
[d] Fondazione Policlinico Universitario Campus Bio-Medico di Roma, Via Alvaro del Portillo, 200, 00128 Rome, Italy
[e] Department of Neurology and Psychiatry, Sapienza" University of Rome, Italy
[f] Epilepsy Center, Neurology Unit. Department of Systems Medicine, University of Rome Tor Vergata, Italy

ARTICLE INFO

Keywords:
quantitative EEG
Lacosamide
Drug-naive
Focal epilepsy

ABSTRACT

Objective: This study investigates pharmaco-EEG changes induced by Lacosamide (LCM) in drug-naive people with focal epilepsy (PwE) and explores the association between quantitative EEG (qEEG) and long-term clinical outcome.

Methods: We retrospectively identified 28 PwE and 25 healthy controls (HC). PwE were classified as seizure-free (SF) or non-seizure-free (NSF) after two years of LCM. EEGs were acquired before and ~ 6 months after LCM. Power spectral density (PSD), amplitude-envelope correlation (AEC), and graph-theoretical metrics were compared between PwE and HC. Logistic regression was employed to examine the association between long-term outcomes (two-year seizure freedom) and qEEG metrics, in combination with clinical variables (sex, aetiology, seizure type, baseline EEG).

Results: LCM did not significantly modify global-averaged qEEG metrics ($p > 0.05$). Theta-band PSD was higher in PwE than HC. PwE exhibited higher alpha-band betweenness centrality (BtwC) than HC only before LCM ($p = 0.007$). Alpha-band BtwC provided the greatest discriminative value for seizure freedom (accuracy = 0.86; area under the curve [AUC] = 0.88).

Conclusions: Although no significant differences were observed between pre- and post-LCM conditions, alpha-band BtwC showed a return toward a more physiological state after treatment, suggesting partial network normalization. Combining qEEG with clinical data improved long-term outcome discrimination, with alpha-band BtwC as the most relevant feature.

Significance: Graph-theoretical qEEG metrics offer additional insight into LCM's neurophysiological effects in focal epilepsy.

1. Introduction

Lacosamide (LCM) is a third-generation antiseizure medication (ASM) approved for the treatment of focal-onset seizures with or without secondary generalization and primary generalized tonic-clonic seizures in both adults and adolescents (Yang et al., 2021). LCM has gained clinical relevance due to its unique mechanism of action: it selectively enhances the slow inactivation of voltage-gated sodium

Abbreviations: AEC, Amplitude Envelope Correlation; AEs, Adverse Effects; ASMs, Anti-Seizure Medications; AUC, Area Under the Curve; BtwC, Betweenness Centrality; CBZ, Carbamazepine; CC, Closeness Centrality; DC, Degree Centrality; EC, Eigenvector Centrality; FC, Functional Connectivity; FFT, Fast Fourier Transform; HC, Healthy Controls; ILAE, International League Against Epilepsy; IQR, Inter-Quartile Range; LCM, Lacosamide; MEG, Magnetoencephalography; MST, Minimum Spanning Tree; NPV, Negative Predictive Value; NSF, Non–Seizure-Free; OXC, Oxcarbazepine; PPV, Positive Predictive Value; PSD, Power Spectral Density; PwE, People with Epilepsy; ROC, Receiver Operating Characteristic; SF, Seizure-Free; VGSCs, Voltage-Gated Sodium Channels.

* Corresponding author at: Cumming School of Medicine, University of Calgary, Calgary, Canada.
E-mail address: lorenzo.ricci@ucalgary.ca (L. Ricci).

https://doi.org/10.1016/j.clinph.2026.2111506
Accepted 15 January 2026
Available online 17 January 2026

channels (VGSCs), in contrast to traditional ASMs that primarily affect fast inactivation (Errington et al., 2008). This distinctive pharmacological profile contributes to its favorable tolerability and reduced interaction potential, making LCM a viable option for people with epilepsy (PwE) (Li et al., 2020).

A recent systematic review and *meta*-analysis involving more than 12,000 patients confirmed that LCM is generally safe and well-tolerated, with an overall adverse event (AE) rate of 38.7 % and a discontinuation rate due to AEs of 10.8 % (Yang et al., 2021). The most frequently reported AEs were central nervous system-related, including sedation, dizziness, and fatigue, followed by gastrointestinal symptoms such as nausea and vomiting. When compared with other sodium channel blockers like carbamazepine (CBZ) and oxcarbazepine (OXC), LCM demonstrated a more favorable safety profile (Chung, 2010).

While LCM's efficacy and tolerability are well established, its impact on cortical network dynamics has yet to be fully elucidated. The use of pharmaco-electroencephalography (pharmaco-EEG), the quantitative analysis of EEG (qEEG) alterations induced by pharmacological treatments, has emerged as a valuable tool to explore the cortical effects of ASMs (Höller et al., 2018). qEEG can detect drug-related changes in cortical rhythms and network connectivity, offering insights into mechanisms of action, therapeutic efficacy, and potential neurocognitive side effects (Ricci et al., 2021). qEEG has previously been employed to characterize the neurophysiological effects of various ASMs, including perampanel, eslicarbazepine acetate, and brivaracetam (Lanzone et al., 2021; Pellegrino et al., 2018; Ricci et al., 2022). However, the qEEG profile of LCM remains largely unexplored.

In this context, the present study aims to assess the effects of LCM on cortical activity and functional connectivity (FC) using resting-state EEG in a population of drug-naive PwE. We also aim to assess whether qEEG measures can be associated with long-term clinical outcomes in patients with focal epilepsy starting LCM therapy. We hypothesize that qEEG analysis can reveal specific alterations in EEG activity and FC following the initiation of LCM therapy. To test this hypothesis, we conducted a multicenter retrospective qEEG study comparing EEG recordings obtained before and after LCM initiation in a cohort of PwE and in a population of healthy controls (HC).

2. Materials and methods

2.1. Enrollment and clinical evaluation

We retrospectively reviewed data from 28 drug-naive PwE and 25 HC. Subjects were enrolled retrospectively at the epilepsy clinic of the Department of Human Neurosciences at Policlinico Umberto I University Hospital in Rome, the Department of Systems Medicine at the University of Rome Tor Vergata, and the "Fondazione Policlinico Campus Bio-Medico" in Rome between January 2010 and March 2025.

We included PwE who met the following inclusion criteria: (i) diagnosis of new focal-onset epilepsy according to the International League Against Epilepsy (ILAE) diagnostic criteria (Beniczky et al., 2025); (ii) $>$ 18 years old; (iii) no previous ASM therapy (drug-naïve patients); (iv) the patients underwent LCM as first antiseizure medication; (v) at least two standard EEGs performed before ($<$30 days; Pre-LCM) and approximately 6 months after LCM introduction (Post-LCM; range: 5.5–6.5 months), considering LCM as monotherapy; (vi) for each recording, a minimum of three minutes of artifact-free resting-state EEG were selected for analysis. Segments containing eye movements, muscle artifacts, or electrode noise were visually identified and excluded before analysis; (vii) two-years post medication clinical follow-up was available.

The exclusion criteria were: (i) PwE taking neuroactive drugs other than LCM; (ii) PwE abruptly discontinued ASMs or introduced new ASMs during the interval between the two EEG recordings; (iii) clinical seizure/s in the 24 h before the EEGs; (iv) EEG signs of drowsiness or sleep and excessive sleepiness before EEG recording ($>$3 on the Stanford Sleepiness Scale).

Seizure outcome was assessed during the last clinical outpatient follow-up visit, based on patient self-report and/or prospective seizure diary review. PwE were classified as seizure-free (SF) if they reported complete absence of seizures during the follow-up period, whereas patients reporting any ongoing seizures during the follow-up period were classified as non-seizure-free (NSF).

The EEG data of HC have been previously used in other studies conducted by our group. In particular, healthy subjects were recruited from hospital staff and volunteers and were interviewed by a neurologist to exclude conditions that could bias the study. The selection criteria for healthy controls were: (i) age $>$ 18 years; (ii) no current substance abuse or significant medical or psychiatric conditions; (iii) no psychotropic or neuroactive drug assumptions (Ricci et al., 2021).

The study protocol received approval from the ethics committee of Policlinico Umberto I Ethic Board-Rome, Campus Bio-Medico University Hospital Foundation Ethic Board-Rome, and "Sapienza" University of Rome Ethic Board-Rome. All procedures were performed in agreement with the 1964 Helsinki Declaration and its later amendments.

2.2. EEG recording and quantitative EEG analysis

EEG recording was performed using the same methodology as in previous works from our group (Pellegrino et al., 2018; Ricci et al., 2021). Nineteen-channel EEG data were recorded with a Micromed recorder (Micromed, Modigliano Veneto, IT). Electrodes were positioned following the international 10–20 system (Fp1, Fp2, F3, F4, C3, C4, P3, P4, F7, F8, T3, T4, T5, T6, O1, O2, Fz, Cz, Pz). The reference electrode was on FPz, while the ground was on FCz. Electrode impedance was maintained below 5 kOhm. In order to reduce inter-center variability, the sampling rate was set to 256 Hz. Resting-state EEG recordings, lasting 15 min, were conducted with patients and healthy controls seated in a comfortable armchair, with closed eyes and in a quiet environment (Ricci et al., 2021). qEEG analysis was performed using the Brainstorm toolbox (Tadel et al., 2011) and in-house Matlab code. Two experienced neurophysiologists (M.S., L.R.) selected, from each EEG, a total of 180 s of continuous epoch free of relevant artifacts or epileptiform abnormalities to be used for further analysis (Babiloni et al., 2020). Brainstorm was utilized for data pre-processing, which include: (i) a visual review by two experienced neurophysiologists to exclude potential interictal and ictal epileptiform activities; (ii) removal of Direct Current offset; (iii) 50-Hz notch filter for powerline noise; (iv) band-pass filter ranging from 1 to 70 Hz; (v) re-referencing of EEG to the common average; (vi) rectification of pulse and eyeblink artifacts through Independent Component Analysis (Ricci et al., 2021).

2.3. EEG power spectrum

We assessed the influence of LCM on resting-state EEG by estimating power spectral density (PSD). We derived mean band power by averaging the PSD for the following frequency bands: (i) Delta δ: 2–4 Hz; (ii) Theta θ: 5–7 Hz; (iii) Alpha α: 8–12 Hz; (iv) Beta β: 13–29 Hz; and Gamma **γ**: 30–60 Hz. We computed PSD measurements per channel and then averaged across all channels to obtain a global cortical activity index. For each channel, we used Welch's method (2-second, non-overlapping windows). We computed a Fast Fourier Transform (FFT) for every window, formed the periodogram (squared magnitude with Welch normalization), and averaged across windows to obtain the PSD. This procedure gives a 0.5 Hz frequency resolution.

2.4. EEG connectivity

In order to assess the influence of LCM on resting-state EEG, connectivity matrices were calculated using Amplitude Envelope Correlation (AEC), a frequency-specific, non-directional measure of FC based on amplitude coupling, reflecting large-scale neural integration (Godfrey

and Singh, 2021; Lachaux et al., 1999). AEC was computed for all the frequency bands as aforementioned. To obtain a measure of global connectivity index, we averaged AEC measures across all channels per frequency band. The EEG pipeline and study flowchart are summarized in Fig. 1.

2.5. Graph–theoretical analysis

To investigate global properties of functional brain networks, we applied graph theory using the Minimum Spanning Tree (MST) algorithm on FC matrices. The network analysis was conducted with an in-house MATLAB code. The MST is a subgraph derived from a weighted undirected connectivity matrix that links all nodes in the network without forming any cycles or closed paths, preserving only the strongest and most meaningful connections while ensuring that all nodes (electrodes) remain connected without forming any cycles (van Dellen et al., 2018). By definition, it consists of m = N − 1 edges, where N represents the total number of nodes. Graph theory metrics were calculated on the whole network in every subject, for each epoch and frequency band, based on AEC global connectivity. We quantified MST topology with four centrality measures: betweenness centrality (BtwC), degree centrality (DC), closeness centrality (CC), and eigenvector centrality (EC). For each frequency-specific MST, node-wise values were computed and averaged across nodes to obtain a global index per band.

On a tree the geodesic between any two nodes is unique; therefore, BtwC reduces to the normalized count of node pairs whose path traverses node i:

$$BtwC_i = \frac{1}{(N-1)(N-2)} \sum_{h \neq j\, h \neq i,\, j \neq i} 1\{i \in path(h,j)\}$$

BtwC quantifies the contribution of a node to global integration and was employed to test LCM-related changes in long-range routing.

CC uses geodesic distance on the MST and is defined as:

$$CC(i) = \frac{N-1}{\sum_k d_{ik}}$$

where d_{ik} is the number of edges on the unique path between i and k. It summarizes how efficiently a node can reach all others (Bröhl and Lehnertz, 2022).

DC is defined as:

$$k_i = \sum_j a_{ij}$$

with a_{ij} the binary adjacency of the tree. It captures local branching and hubness and was used to assess changes in focal or distributed hubs.

EC is given by the dominant eigenvector of the MST adjacency,

$$Av = \lambda_{max} v$$

with $EC_i = v_i$. It reflects hierarchical influence through connections to well-scored neighbors and was used to characterize organization beyond raw degree (Bröhl and Lehnertz, 2022).

All metrics were computed with the same pipeline in every band and summarized as global indices (van Dellen et al., 2018).

2.6. Statistical analysis

We performed statistical analysis using the *R statistical packages* and *Matlab R2024b (MathWorks)*. Significance level was set at 0.05. The distribution of clinical and demographic data was checked using the Shapiro-Wilk test. Non-normally distributed data were reported using the median, the range from minimum to maximum, and the interquartile range (IQR). Normally distributed data were reported as mean value ± SD. Patients' clinical characteristics and LCM-induced modifications in PSD and global connectivity were compared between SF and NSF

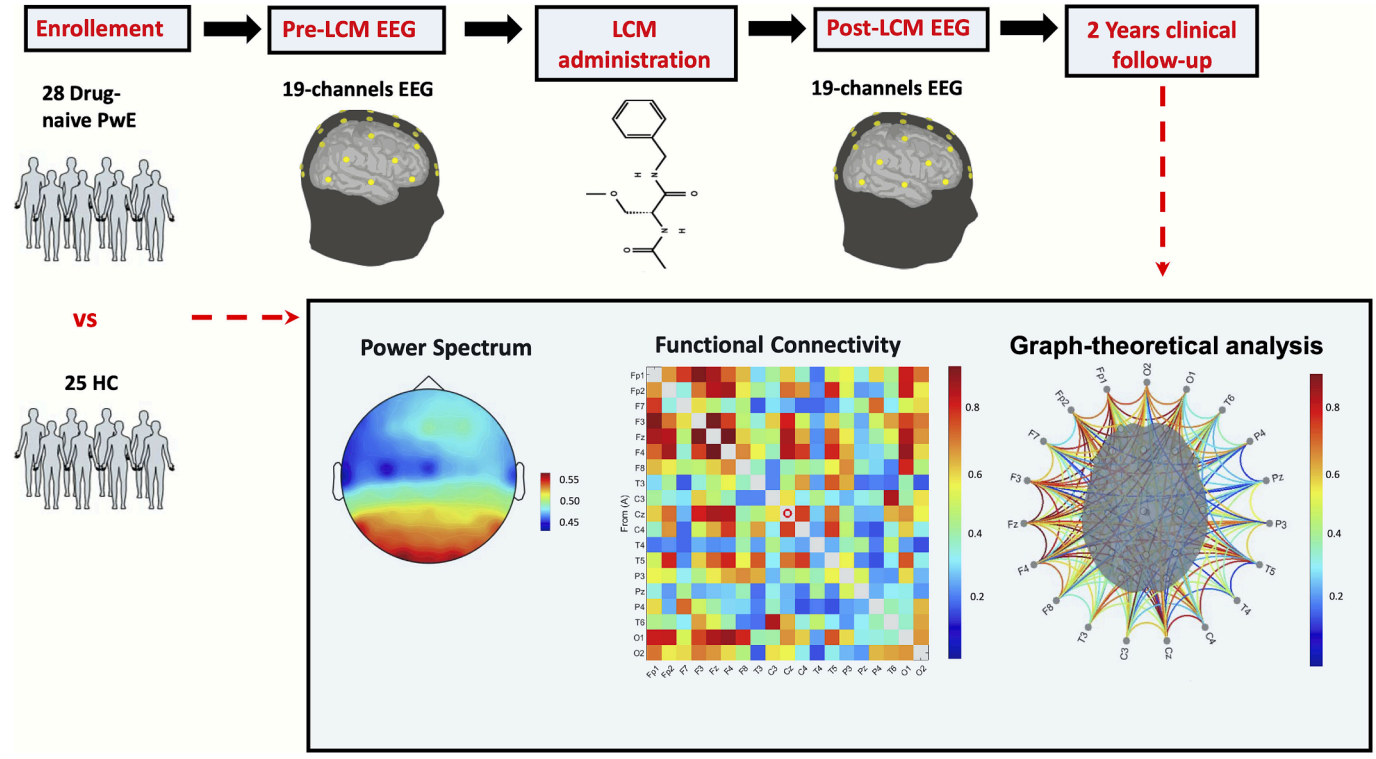

Fig. 1. Methodological Pipeline and study flowchart. The study involved two groups: 28 drug-naive adult people with focal-onset epilepsy (PwE) and 25 healthy controls (HC). All patients underwent 19-channel EEG before and after approximately 6 months of Lacosamide (LCM) treatment. The 19-channel EEG data of the HC were also analyzed. We analyzed quantitative EEG features, including power spectral density (PSD) and functional connectivity (FC) and graph-theoretical metrics across all standard frequency bands (delta to gamma). Long-term clinical follow-up (2 years) was conducted for all patients to enable comparison of EEG features over time.

patients using the χ^2 test for categorical variables and the Mann-Whitney *U* test for continuous variables.

To test the effect of LCM therapy on the EEG global cortical activity (PSD) and global connectivity (AEC), we performed a rank-based Kruskal-Wallis test with *Bands* (five levels: Delta, Theta, Alpha, Beta, Gamma), *Group* (three levels: pre-LCM, post-LCM, HC) and the interaction term (*Group* vs. *Bands*). P-values were obtained by likelihood ratio tests. In cases of significant interactions, we performed post-hoc tests with *Group* contrasts based on Dunn's Comparison method, separately for each frequency band. We also examined the impact of LCM therapy on EEG graph metrics by conducting Kruskal-Wallis tests on centrality measures derived from AEC-based global connectivity across different frequency bands, using *Group* as the between-subjects factor and *Group* × *Band* as the interaction factor. Post-hoc analysis was corrected for multiple comparisons using the Bonferroni method.

2.7. Association between qEEG and clinical outcome

A multivariate logistic regression model was performed to assess whether quantitative EEG measures could predict patients' long-term clinical outcome and whether EEG analysis added predictive value beyond clinical variables. To prevent multicollinearity, variables with a Variance Inflation Factor (VIF) of 5 or higher were excluded. The EEG model included graph theory metrics computed for each frequency band: BtwC, CC, DC, EC (Shi et al., 2025). The clinical model included sex, aetiology (structural vs. non-structural), seizure type (focal to bilateral tonic-clonic seizures, focal seizures with preserved consciousness, focal seizures with impaired consciousness), and baseline EEG findings (presence or absence of interictal epileptiform discharges) (Ricci et al., 2021). The combined model included both clinical and qEEG features.

The saliences of qEEG metrics and clinical variables were represented by odds ratios (ORs) along with the 95 % confidence interval (CI). CI was derived from the profile likelihood function test. For each model, we generated receiver operating characteristic (ROC) curves and areas under the curve (AUCs). Each model was compared using both the likelihood-ratio test and the DeLong test. The likelihood-ratio test assessed whether adding EEG variables significantly improved the overall model fit compared to the clinical model alone. The DeLong test evaluated whether the AUC of the combined model was significantly different from that of the clinical model. This analysis was conducted on resting-state EEGs before (pre-LCM) and after LCM introduction (post-LCM). We determined specificity, sensitivity, area under the curve (AUC), positive predictive value (PPV), negative predictive value (NPV), and Accuracy for each model. For each measure, 95 % CI was calculated using the DeLong non-parametric method for AUCs and the Wilson score method for binomial proportions. The Youden index determined the optimal probability threshold for each model.

3. Results

3.1. Clinical data and grouping

Twenty-eight PwE (13 females) were included in the study. Clinical and demographic characteristics of our cohort are reported in Table 1. The mean age at the time of LCM introduction was 51.4 ± 18.3 years

Table 1
Patients Clinical Information and Outcome.

Patient	Age (ys)	Sex	Aetiology	Epilepsy Duration (ys)	Seizure Type	Seizure Frequency	Epileptogenic Focus*	Adverse Events	Outcome
1	45	F	Unknown	3	FTB	Yearly	Right CT	Yes (balance impairment)	SF
2	56	M	Unknown	4	FTB	Single episode	Right TP	No	SF
3	63	F	Unknown	3	FTB	Yearly	Left FT	No	NSF
4	69	M	Structural (Ischemic Stroke)	7	FIC	Monthly	Left FT	No	SF
5	66	M	Unknown	8	FIC, FTB	Yearly	Left CT	No	NSF
6	64	F	Unknown	3	FTB	Single episode	Left TP	Yes (balance impairment)	NSF
7	36	F	Structural (periventricular nodular heterotopia)	1	FTB	Yearly	Right FCT	No	NSF
8	45	M	Structural (Ischemic Stroke)	8	FTB	Monthly	Right T	No	SF
9	30	M	Structural (periventricular nodular heterotopia)	10	FIC	Weekly	Left T	Yes (drowsiness)	SF
10	48	M	Structural (post neurinoma resection)	15	FIC	Monthly	Left FT	No	NSF
11	82	F	Unknown	3	FPC	Yearly	Left FCT	No	SF
12	56	F	Structural (Ischemic Stroke)	4	FIC	Yearly	Left TP	No	NSF
13	54	M	Unknown	4	FIC, FTB	Monthly	Right CP	No	NSF
14	29	M	Structural (cavernous malformation)	0	FPC, FTB	Daily	Left T	Yes (nausea, balance impairment)	SF
15	72	M	Unknown	6	FPC	Weekly	Right CT	No	NSF
16	25	F	Unknown	1	FTB	Yearly	Left FT	No	SF
17	70	M	Unknown	3	FTB	Weekly	Right FCT	No	NSF
18	70	F	Structural (Ischemic Stroke)	2	FIC, FTB	Monthly	Right FCT	No	NSF
19	73	M	Unknown	7	FIC	Yearly	Left T	No	SF
20	80	M	Unknown	5	FTB	Yearly	Right FT	No	SF
21	37	F	Structural (cortical dysplasia)	19	FIC	Weekly	Right T	No	NSF
22	28	F	Structural (arteriovenous malformation)	3	FTB, FIC	Monthly	Left TP	No	NSF
23	44	F	Unknown	24	FTB	Yearly	TO Bil	No	NSF
24	36	M	Structural (Ischemic Stroke)	21	FTB, FIC	Yearly	Right CT	No	NSF
25	24	F	Unknown	1	FTB, FPC	Monthly	Left T	No	SF
26	25	M	Unknown	11	FTB	Monthly	–	No	SF
27	68	F	Unknown	43	FIC	Yearly	FT Bil	No	SF
28	44	M	Structural (Cyst)	23	FIC	Weekly	Right T	No	NSF

Ys = years; M = Male; F = Female; FIC: Focal Impaired Consciousness; FPC: Focal Preserved Consciousness; FTB: Focal To Bilateral tonic-clonic; Bil. = Bilateral; T = Temporal; FCT = Fronto-Centro-Temporal; CT = Centro-Temporal; CP = Centro-Parietal; FT = Fronto-Temporal; TP = Temporo-Parietal; TO = Temporo-Occipital; SF = Seizure-Free; NSF = Non-Seizure-Free; * Presumed epileptogenic focus based on anatomo-electro-clinical correlations.

(range: 24–82 years). Thirteen PwE were classified as SF after LCM (46.4 %), whereas 15 were NSF (53.6 %). Twelve patients (43 %) presented a structural cause of their epilepsy. Four patients (14 %) experienced non-serious adverse events related to LCM therapy. Twenty-five healthy subjects (12 females) were considered the control group. The mean age was 58.6 ± 18.7 years (range: 28–83 years). The mean age did not significantly differ between the epilepsy and control groups (p = 0.16). The median duration of epilepsy was 7.9 years for SF (IQR = 3–8 years) and 9.3 years for NSF (IQR = 3–17 years), with no significant differences between the two groups ($p = 0.72$). No significant associations were found between the presence of structural etiology and clinical outcome (30.7 % for SF and 53.3 % for N-SF; $p = 0.412$).

3.2. Comparison between epilepsy and control groups: PSD results

The Kruskal-Wallis test revealed a significant difference in the factor *Group* between PwE and HC ($p < 0.001$). Post-hoc tests revealed that PwE had significantly higher PSD theta values compared to HC, both before (pre-LCM vs. HC; z = 3.11; $p < 0.005$) and after LCM therapy (post-LCM vs. HC; z = 3.72; $p < 0.001$). No significant differences were found in the comparison of PSD values between pre- and post-LCM (p = 0.532; Fig. 2).

3.3. Graph theory metrics

The Kruskal-Wallis test revealed a significant main effect of the factor *Group* on mean BtwC, derived from AEC global connectivity ($p = 0.027$). Post-hoc analysis showed that PwE exhibited higher alpha band BtwC compared to HC only before LCM therapy (pre-LCM vs. HC; z = -2.67; p = 0.007). No significant differences were found after LCM therapy (post-LCM vs. HC; z = -1.22; p = 0.22) or in the comparison of BtwC alpha values between Pre and Post-LCM (pre-LCM vs. post-LCM; z = 1.49; p = 0.13; Fig. 3). The Kruskal-Wallis test did not reveal any significant effect of factor *Group* on the other tested centrality measures for each of the five frequency bands tested.

3.4. Logistic regression and clinical association of quantitative EEG analysis

Among the EEG-derived predictors, only pre-LCM mean BtwC derived from AEC global connectivity showed a statistically significant association with long-term clinical outcome. The results of multiple logistic regression and cross-validated ROC curve analysis are reported in Fig. 4. Mean BtwC in the alpha band performed on pre-LCM EEG recordings correlated with seizure outcome at the 2-year follow-up, achieving an overall accuracy of 0.86 (95 % CI: 0.70–0.94), AUC 0.88 (95 % CI: 0.74–1.00), sensitivity 0.85 (95 % CI: 0.58–0.96), specificity 0.87 (95 % CI: 0.62–0.96), PPV 0.85 (95 % CI: 0.60–0.96) and NPV 0.87 (95 % CI: 0.62–0.96) for the combined clinical and EEG model; and an overall accuracy of 0.71 (95 % CI: 0.54–0.85), AUC 0.71 (95 % CI: 0.51–0.90), sensitivity 0.77 (95 % CI: 0.50–0.92), specificity 0.67 (95 % CI: 0.42–0.85), PPV 0.67 (95 % CI: 0.42–0.85) and NPV 0.77 (95 % CI: 0.50–0.92) for the clinical model alone. None of the clinical predictors were excluded due to low VIP levels.

Most clinical and EEG variables did not significantly improve the discriminative performance of the combined model compared to the clinical model alone (p > 0.05 for all variables). However, pre-LCM mean BtwC in the alpha band was strongly and inversely associated with seizure outcome (OR = 0.001; p = 0.02), indicating that higher baseline BtwC values in the alpha band were associated with a lower probability of achieving seizure freedom. Aetiology also showed a borderline inverse association with seizure outcome (OR = 0.07; p = 0.05). The complete results for each clinical and EEG feature are reported in Supplementary Table 1.

The combined Clinical + EEG model provided a significantly better fit than the clinical model alone (LRT $\chi^2(1) = 9.4$, p = 0.002) and achieved higher apparent discriminative performance (AUC = 0.88 [95 % CI 0.74–1.00]) compared to the Clinical model (AUC = 0.71 [95 % CI 0.55–0.87]).

The difference in AUCs was also statistically significant (DeLong test, Z = 1.98, p = 0.04).

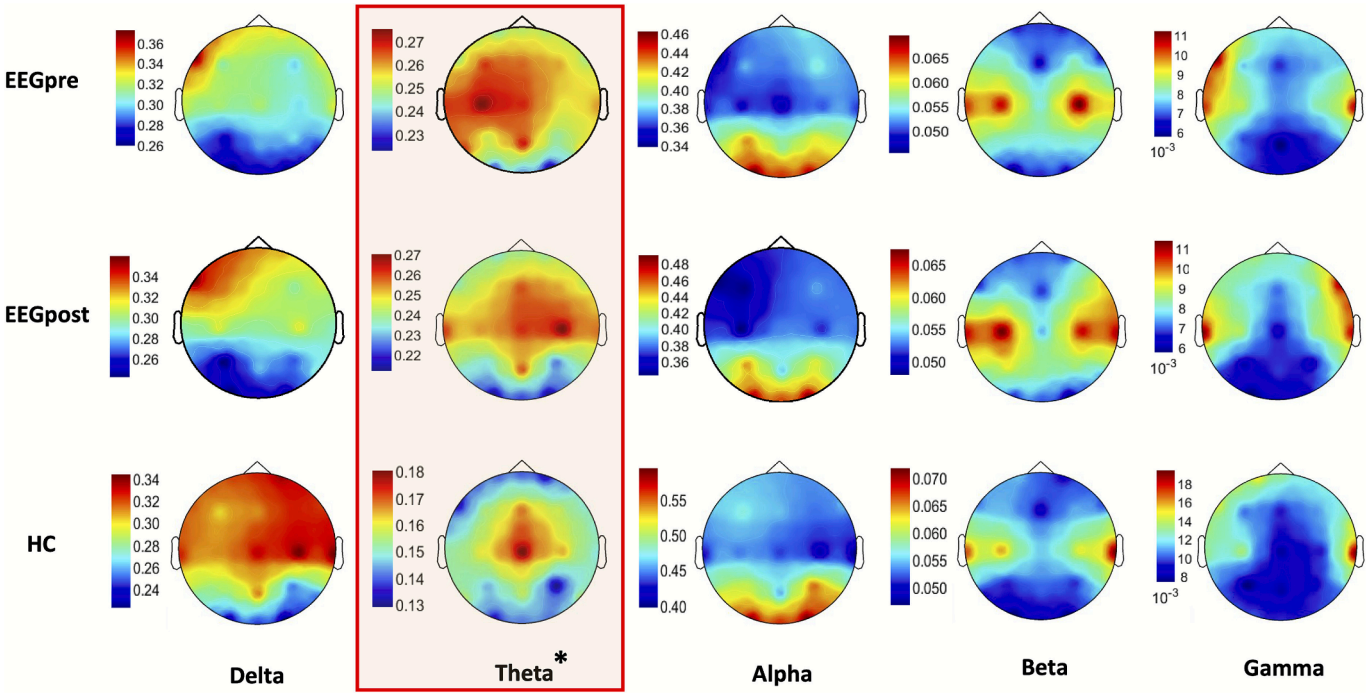

Fig. 2. EEG power spectral density (PSD). PSD scalp distribution expressed as average across channels. Pre EEG performed before the initiation of Lacosamide (LCM) therapy. Post EEG performed after approximately 6 months of LCM therapy. *p < 0.05.

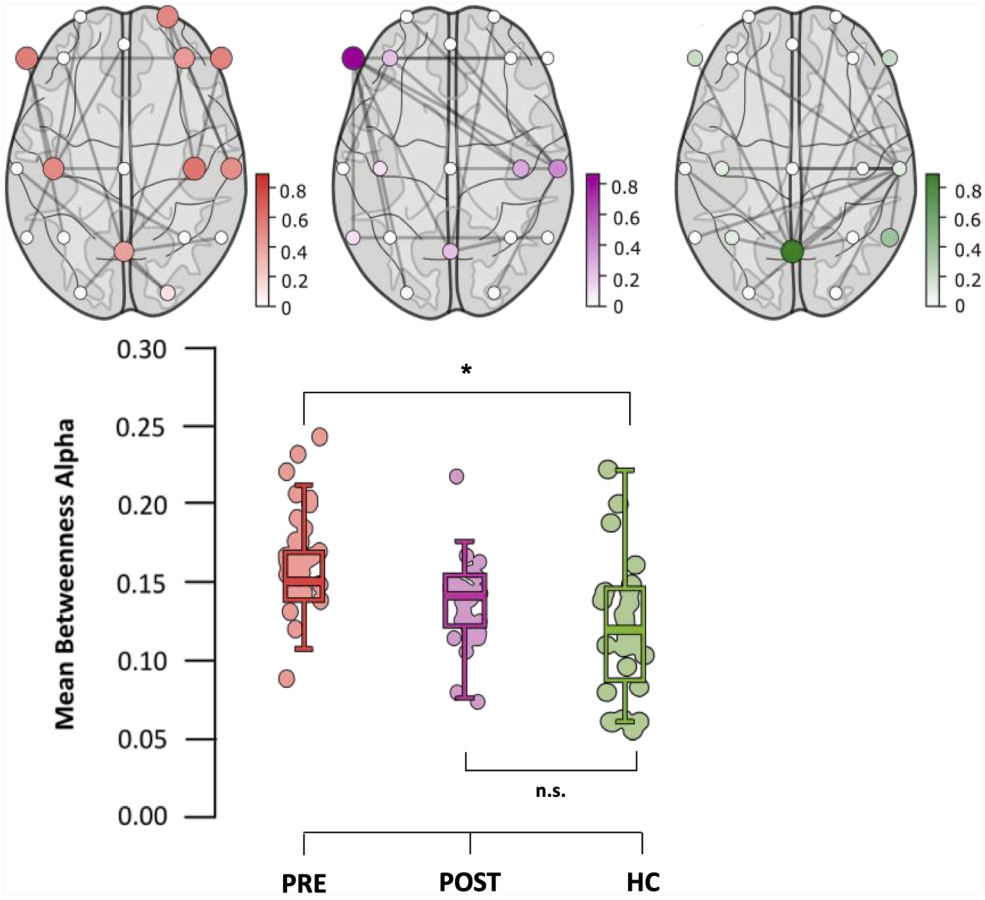

Fig. 3. EEG Mean Betweenness Centrality (BtwC). Superior panel displays graph configuration of the Mean Betweenness Centrality (BtwC) in the alpha band. The size of each electrode (node) is directly proportional to the BtwC level of each channel. Lines represent the edges connecting each node. Inferior panel displays box plot distributions and scatter plot distributions of BtwC EEG in the alpha band across Groups (PRE, POST and HC). *p < 0.05. n.s. = non-significant.

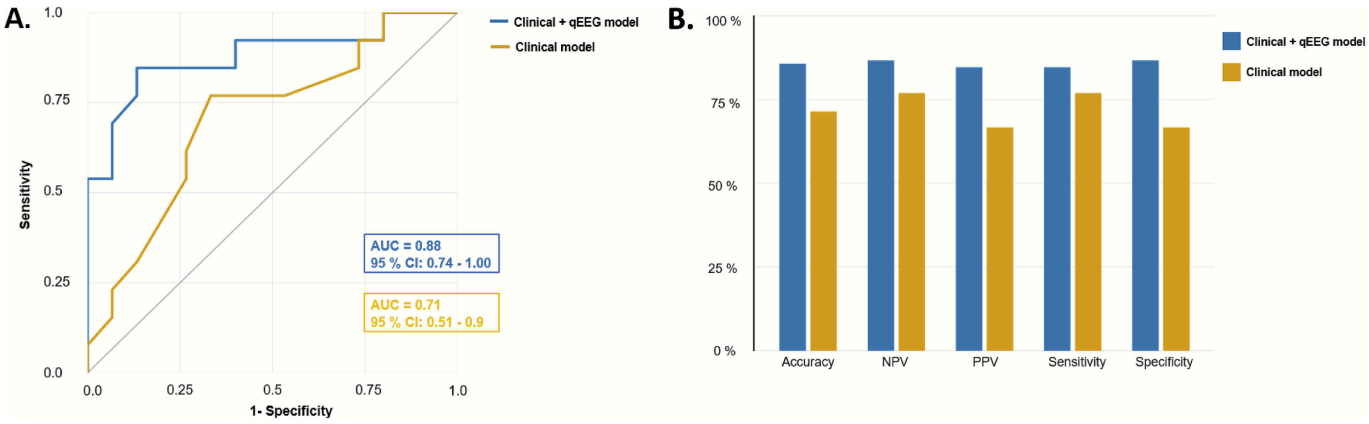

Fig. 4. Logistic regression model. A. Receiver operating characteristic (ROC) curves of the clinical and combined (clinical + qEEG) models based on pre-LCM resting-state EEG, including alpha-band BtwC. The combined model achieved an AUC of 0.88 [95 % CI 0.74–1.00], while the clinical model showed an AUC of 0.71 [95 % CI 0.51–0.90]. B. Bar plots showing model performance metrics. Bars (blue = clinical + qEEG model; yellow = clinical model). Accuracy, NPV, PPV, Sensitivity, and Specificity are computed at the optimal Youden cut-off.

4. Discussion

In our study, we analyzed the effects of LCM monotherapy in drug-naive PwE compared to HC, and whether qEEG measures can be associated with long-term clinical outcomes. The main findings of the study can be summarized as follows: (i) LCM does not significantly modify global-averaged qEEG measures (PSD or connectivity metrics); (ii) PwE show increased EEG PSD in the theta-band compared to HC; (iii) Alpha-band BtwC decreases after treatment, with no difference from HC, suggesting partial normalization of network topology; (*iv*) The integration of qEEG metrics into a clinical model improved long-term outcome discrimination.

4.1. LCM does not induce significant alterations in resting-state EEG

We examined the impact of LCM monotherapy on qEEG features in PwE. We found no significant differences in global-averaged qEEG parameters (PSD, AEC-derived Graph Theory metrics) across any of the tested frequency bands between pre- and post-LCM. This might be related to LCM's established safety neurophysiological tolerability profile. Indeed, our findings align with previous reports on the effects of LCM on qEEG activity, indicating that LCM does not cause significant changes in resting-state EEG (Giorgi et al., 2013).

In contrast, studies involving older-generation sodium channel blockers, such as CBZ and OXC, have demonstrated a notable reduction in the PSD within the alpha band (Frost et al., 1995; Giorgi et al., 2013). The decrease in alpha-band PSD values has been interpreted as reflecting the sedative and cortical-depressant effects of these agents, which tend to suppress spontaneous cortical oscillations and decrease network synchronization (Assenza et al., 2017). The possible explanation for this finding lies in their distinct mechanism of action on VGSCs. VGSCs play a key role in initiating and propagating action potentials. Drug-induced VGSC inactivation comprises two distinct processes: fast and slow inactivation. Fast inactivation is crucial for terminating action potentials and defining the refractory period. Slow inactivation contributes to the modulation of overall neuronal excitability by increasing the threshold required for action potential initiation. Traditional VGSC-blocking antiseizure medications, such as phenytoin, CBZ and OXC, primarily work by increasing fast inactivation of VGSCs (Rogawski and Löscher, 2004), leading to phasic inhibition. Unlike older sodium channel blockers, LCM exerts its anti-seizure effect by selectively enhancing the slow inactivation of VGSCs, which occurs within seconds to minutes. By stabilizing VGSCs in the slow inactivated state, LCM prevents their rapid recovery to an active state between bursts, thereby limiting sustained bursting activity under pathological conditions (Errington et al., 2008). This results in a tonic, state-dependent inhibition that preferentially targets neurons undergoing sustained and pathological depolarization. Therefore, LCM's mechanism of action may offer a reasonable explanation for the lack of significant changes in PSD and FC features across different frequency bands. This notion also aligns with the absence of subjectively reported significant adverse effects in our cohort during the follow-up period, particularly drowsiness or cognitive impairment.

4.2. Increased Theta-Band PSD suggests interictal network dysregulation in epilepsy

The use of PSD analysis enabled us to characterize EEG activity by frequency-specific oscillatory components, providing a quantitative framework for comparing signal power across groups and for identifying changes in cortical rhythms associated with epilepsy. In our study, the EEG power spectrum in PwE exhibits widespread increases in the theta band compared to HC. This result aligns with prior studies reporting slow-wave power enhancement as a key feature of resting-state EEG in PwE (Lanzone et al., 2021; Ricci et al., 2021). It has been widely reported that theta oscillations are linked to drowsiness and the structural and functional reorganization of brain networks through long-lasting plasticity, including memory formation, attention, and spatial navigation (Assenza et al., 2017a, 2017b; Tan et al., 2024). However, the presence of delta and theta rhythms during wakefulness is considered a sign of neuropathological processes, including abnormal activity originating in epileptogenic regions (Cassidy et al., 2020; Pellegrino et al., 2017). To provide an explanation for the neurobiological mechanisms underlying our findings, it is plausible that thalamic dysregulation plays a crucial role. It is widely recognized that the thalamic nuclei modulate long-range synchrony in both focal and generalized epilepsies, and an impairment in the thalamocortical network has been associated with seizure generation (Chiosa et al., 2017; Lüttjohann and van Luijtelaar, 2022). The altered theta activity may stem from thalamocortical circuits impaired by an imbalance between excitatory and inhibitory processes, a well-documented feature of epilepsy pathophysiology that may underlie the observed network changes (Assenza et al., 2020; Englot et al., 2015). In conclusion, the observed increase in theta-band PSD among PwE may signal an underlying disruption of neural circuits. It could reflect either a compensatory response to epileptic network dysfunction or a consequence of chronic seizure burden (Ricci et al., 2022).

4.3. Graph metrics: Brain network modification induced by LCM

The human brain is arguably among the most sophisticated network systems in the natural world. It can be conceptualized as a complex, network-based algorithm that delineates the parameters defining the brain's overarching organizational architecture. Disruptions in these networks are recognized as key contributors to neurological dysfunction. Epilepsy, characterized by unpredictable and sudden paroxysmal neuronal synchronization, exemplifies this model. Previous studies have employed graph theory on EEG data to investigate brain network organization across different conditions, focusing on possible changes in global or local metrics (Vecchio et al., 2014, 2017). A brain graph theory network is a mathematical model of brain architecture, comprising nodes (vertices) and edges (links) that connect them. Nodes typically represent brain regions, while edges reflect anatomical, functional, or effective connections (Friston, 1994; Rubinov and Sporns, 2010). Over time, the concept of hubness has gained increasing attention. Hubs are nodes of high strategic importance, playing a crucial role in facilitating efficient information integration across the network (van den Heuvel and Hulshoff-Pol, 2010; Ridley et al., 2015). Thus, injury to these nodes is expected to exert a greater impact on global network organization and integrative processes than lesions confined to peripheral nodes (van den Heuvel and Sporns, 2013). Graph-theoretical metrics used to identify hubs typically include high degree or strength, high centrality, short characteristic path length, and low clustering coefficient (van den Heuvel and Hulshoff Pol, 2010). The role of brain network hubs in focal epilepsy remains unclear. Given their central role in information transfer, hubs may also become bottlenecks under pathological conditions. In fact, increased hubness in certain nodes might indicate maladaptive routing of information, particularly in focal epilepsy, resulting in decreased network efficiency and impaired communication. As a result, such nodes could serve as potential therapeutic targets (van den Heuvel and Sporns, 2013).

To analyze such central nodes we used graph theory with the MST algorithm on the AEC-derived connectivity matrices: BtwC, CC, DC, EC.

Within an MST framework, network topology is defined by a unique shortest path connecting each pair of nodes. In this context, BtwC directly reflects how much individual nodes serve as essential bridges for information transfer across the network, making it highly sensitive to changes in global network integration and long-distance routing. Conversely, DC primarily reflects local connectivity or hubness, CC reflects how effectively a node can reach all other nodes via shortest paths, and EC measures hierarchical influence through connections to highly connected neighbors. These metrics represent complementary aspects of network organization (local branching, path efficiency, hierarchical structure) and may be less sensitive to specific changes or reorganizations in long-range communication pathways within an MST-constrained topology (van Dellen et al., 2018).

Consistent with this theoretical framework, we observed that only in the alpha band, PwE showed higher BtwC than HC before LCM therapy. According to our data, alpha-band BtwC derived from AEC global connectivity significantly decreased in PwE after LCM therapy, reaching levels that were no longer statistically different from those of HC.

Importantly, although no statistically significant differences were observed between pre- and post-LCM conditions, exploratory analyses showed that alpha-band BtwC values returned toward a more physiological state after treatment. This finding may reflect a transient functional disruption of network organization in focal epilepsy, which appears partially normalized after antiseizure treatment. Interestingly,

the observed "normalization" of BtwC post-LCM may reflect a decrease in pathological network centralization, thereby promoting high network efficiency and preserving effective neural communication. This suggests treatment-related changes, indicating a return to a more physiological network state characterized by the absence of nodal strength or centrality imbalances and a more uniform, symmetric distribution of FC (Ricci et al., 2024).

4.4. Graph-theoretical EEG features and long-term clinical outcome

Our findings provide preliminary evidence supporting the feasibility of using resting-state EEG to quantify treatment-related network changes and clinical response to LCM after long-term ASM therapy. Building on the concept originally introduced by Saletu et al. (1987), qEEG has progressively evolved into a quantitative approach for assessing drug-related effects on brain function across several neurological and psychiatric conditions (Adler et al., 2004; Iosifescu, 2011; Mucci et al., 2006). Within epilepsy research, qEEG approaches have been increasingly applied to explore how ASMs influence FC and large-scale network organization (Engel et al., 2013; Croce et al., 2021; Ricci et al., 2021; Huang and Shen, 1993).

In the present study, we applied a multivariate logistic regression framework to evaluate whether EEG-derived connectivity metrics provide additional information beyond conventional clinical variables in discriminating long-term outcomes in PwE treated with LCM. Two models were tested: a clinical model and a combined model that added qEEG features, including graph theory metrics computed for each frequency band, to the same clinical predictors.

Among all the features examined, only pre-LCM mean BtwC in the alpha band showed a significant association with two-year seizure freedom. When this parameter was added to the clinical model, the combined model demonstrated better discriminative performance than the clinical model alone (AUC = 0.88 [95 % CI 0.74–1.00] vs AUC = 0.71 [95 % CI 0.51–0.90]). The modest but statistically significant improvement observed in the combined model suggests that qEEG measures convey complementary information to clinical predictors. Overall, our findings suggest that graph-theoretical metrics derived from resting-state EEG identify features of the large-scale network organization that are not captured by clinical variables. In particular, alpha-band BtwC appears to reflect treatment-related network reorganization associated with long-term outcomes after LCM therapy. The specific association observed in the alpha band may relate to its role in thalamocortical and fronto-parietal coupling, a key substrate for large-scale integration and functional stability in PwE (Hughes and Crunelli, 2005).

Consistent with previous scalp and intracranial EEG studies linking nodal centrality to seizure networks and surgical outcomes (Gong et al., 2024; Kanai et al., 2024), our data support the potential of alpha-band BtwC as a physiologically meaningful descriptor of network organization. Integrating qEEG-derived connectivity features with standard clinical information may therefore enhance the neurophysiological characterization of treatment effects and contribute to more physiologically grounded models of outcome in focal epilepsy. Nevertheless, these findings should be interpreted with caution, given the exploratory nature of the analysis.

4.5. Limitations and future directions

This study acknowledges several limitations. First, its retrospective and non-randomized design. Although we were able to retrospectively establish a statistical association between qEEG metrics and seizure outcomes, we were unable to evaluate the real-time impact of these analyses on clinical decision-making. Secondly, the sample size of PwE was relatively limited, particularly when stratified by clinical outcome, which may reduce statistical power and generalizability.

Thirdly, the use of a single-center dataset and the absence of an external validation cohort prevent firm conclusions regarding the predictive value of the proposed combined model.

Additionally, our cohort included a heterogeneous spectrum of focal epilepsy types, showing variability in epileptogenic focus, seizure semiology, and aetiology. This heterogeneity may have reduced the sensitivity of focus-specific or lateralization-based qEEG analyses, which limited the ability to detect regional network effects linked to the epileptogenic area.

Finally, it is important to consider that standard EEG offers limited spatial resolution and does not provide full coverage of deep or subcortical brain regions, potentially missing relevant activity.

Future research should include larger, prospectively collected and multicenter cohorts to enable external validation and improve model generalizability. In particular, studies focusing on more homogeneous epilepsy populations will be necessary to further examine lateralized network changes and to better characterize focus-specific patterns of functional reorganization. Incorporating advanced neurophysiological techniques such as high-density EEG and magnetoencephalography (MEG) may further refine the characterization of qEEG markers and clarify their potential role in guiding individualized therapeutic strategies. Efforts to evaluate reproducibility across different recording settings and analytical pipelines will be essential to establish the clinical utility of network-based EEG metrics in treatment monitoring and outcome stratification.

5. Conclusion

This study suggests that LCM monotherapy in drug-naive PwE does not significantly affect qEEG parameters (PSD or FC), supporting its favorable tolerability profile in terms of side effects. Consistent with previous findings, PwE showed increased theta-band PSD values compared with HC, reinforcing its role as a potential biomarker of interictal network dysfunction in epilepsy.

We observed a reduction in alpha-band BtwC in PwE following LCM therapy, suggesting partial normalization of functional network topology. This modulation is consistent with a reorganization toward a more physiological resting-state configuration.

Beyond the characterization of LCM-related network effects, the integration of qEEG metrics with clinical variables offered complementary insight into long-term outcomes, with alpha-band BtwC emerging as the most informative network descriptor. These findings highlight the potential of qEEG as a non-invasive tool to characterize ASM-related network changes and to improve the understanding of treatment effects in focal epilepsy.

Declaration of competing interest

The authors declare that they have no known competing financial interests or personal relationships that could have appeared to influence the work reported in this paper.

Acknowledgment

The author(s) received no specific funding for this work.

Ethical Publication Statement

All the authors confirm that they have read the Journal's position on issues involved in ethical publication and affirm that this report is consistent with those guidelines.

Appendix A. Supplementary data

Supplementary data to this article can be found online at https://doi.org/10.1016/j.clinph.2026.2111506.

References

Adler, G., Brassen, S., Chwalek, K., Dieter, B., Teufel, M., 2004. Prediction of treatment response to rivastigmine in Alzheimer's dementia. J. Neurol. Neurosurg. Psychiatry 75, 292–294.

Assenza, G., Campana, C., Assenza, F., Pellegrino, G., Di Pino, G., Fabrizio, E., et al., 2017a. Cathodal transcranial direct current stimulation reduces seizure frequency in adults with drug-resistant temporal lobe epilepsy: A sham controlled study. Brain Stimul. 10, 333–335. https://doi.org/10.1016/j.brs.2016.12.005.

Assenza, G., Campana, C., Colicchio, G., Tombini, M., Assenza, F., Di Pino, G., et al., 2017b. Transcutaneous and invasive vagal nerve stimulations engage the same neural pathways: In-vivo human evidence. Brain Stimul. 10, 853–854. https://doi.org/10.1016/j.brs.2017.03.005.

Assenza, G., Capone, F., di Biase, L., Ferreri, F., Florio, L., Guerra, A., et al., 2017c. Oscillatory Activities in Neurological Disorders of Elderly: Biomarkers to Target for Neuromodulation. Front. Aging Neurosci. 9. https://doi.org/10.3389/fnagi.2017.00189.

Assenza, G., Lanzone, J., Insola, A., Amatori, G., Ricci, L., Tombini, M., et al., 2020. Thalamo-cortical network dysfunction in temporal lobe epilepsy. Clin. Neurophysiol. 131, 548–554. https://doi.org/10.1016/j.clinph.2019.10.017.

Babiloni, C., Lopez, S., Del Percio, C., Noce, G., Pascarelli, M.T., Lizio, R., et al., 2020. Resting-state posterior alpha rhythms are abnormal in subjective memory complaint seniors with preclinical Alzheimer's neuropathology and high education level: the INSIGHT-preAD study. Neurobiol. Aging 90, 43–59. https://doi.org/10.1016/j.neurobiolaging.2020.01.012.

Beniczky, S., Trinka, E., Wirrell, E., Abdulla, F., Al Baradie, R., Alonso Vanegas, M., et al., 2025. Updated classification of epileptic seizures: Position paper of the International League Against Epilepsy. Epilepsia 66, 1804–1823. https://doi.org/10.1111/epi.18338.

Bröhl, T., Lehnertz, K., 2022. A straightforward edge centrality concept derived from generalizing degree and strength. Sci. Rep. 12, 4407. https://doi.org/10.1038/s41598-022-08254-5.

Cassidy, J.M., Wodeyar, A., Wu, J., Kaur, K., Masuda, A.K., Srinivasan, R., et al., 2020. Low-Frequency Oscillations Are a Biomarker of Injury and Recovery After Stroke. Stroke 51, 1442–1450. https://doi.org/10.1161/STROKEAHA.120.028932.

Chiosa, V., Groppa, S.A., Ciolac, D., Koirala, N., Mişina, L., Winter, Y., et al., 2017. Breakdown of Thalamo-Cortical Connectivity Precedes Spike Generation in Focal Epilepsies. Brain Connect. 7, 309–320. https://doi.org/10.1089/brain.2017.0487.

Chung, S.S., 2010. New treatment option for partial-onset seizures: efficacy and safety of lacosamide. Ther. Adv. Neurol. Disord. 3, 77–83. https://doi.org/10.1177/1756285609355850.

Croce, P., Ricci, L., Pulitano, P., Boscarino, M., Zappasodi, F., Lanzone, J., et al., 2021. Machine learning for predicting levetiracetam treatment response in temporal lobe epilepsy. Clin. Neurophysiol. 132, 3035–3042. https://doi.org/10.1016/j.clinph.2021.08.024.

van Dellen, E., Sommer, I.E., Bohlken, M.M., Tewarie, P., Draaisma, L., Zalesky, A., et al., 2018. Minimum spanning tree analysis of the human connectome. Hum. Brain Mapp. 39, 2455–2471. https://doi.org/10.1002/hbm.24014.

Engel, J., Pitkänen, A., Loeb, J.A., Dudek, F.E., Bertram, E.H., Cole, A.J., et al., 2013. Epilepsy biomarkers. Epilepsia 54 (Suppl 4), 61–69. https://doi.org/10.1111/epi.12299.

Englot, D.J., Hinkley, L.B., Kort, N.S., Imber, B.S., Mizuiri, D., Honma, S.M., et al., 2015. Global and regional functional connectivity maps of neural oscillations in focal epilepsy. Brain 138, 2249–2262. https://doi.org/10.1093/brain/awv130.

Errington, A.C., Stöhr, T., Heers, C., Lees, G., 2008. The investigational anticonvulsant lacosamide selectively enhances slow inactivation of voltage-gated sodium channels. Mol. Pharmacol. 73, 157–169. https://doi.org/10.1124/mol.107.039867.

Friston, K.J., 1994. Functional and effective connectivity in neuroimaging: A synthesis. Hum. Brain Mapp. 2, 56–78. https://doi.org/10.1002/hbm.460020107.

Frost, J.D., Hrachovy, R.A., Glaze, D.G., Rettig, G.M., 1995. Alpha rhythm slowing during initiation of carbamazepine therapy: implications for future cognitive performance. J. Clin. Neurophysiol. 12, 57–63.

Giorgi, F.S., Pizzanelli, C., Pelliccia, V., Di Coscio, E., Maestri, M., Guida, M., et al., 2013. A Clinical-EEG Study of Sleepiness and Psychological Symptoms in Pharmacoresistant Epilepsy Patients Treated with Lacosamide. Epilepsy Res Treat 2013, 593149. https://doi.org/10.1155/2013/593149.

Godfrey, M., Singh, K.D., 2021. Measuring robust functional connectivity from resting-state MEG using amplitude and entropy correlation across frequency bands and temporal scales. Neuroimage 226, 117551. https://doi.org/10.1016/j.neuroimage.2020.117551.

Gong, R., Roth, R.W., Hull, K., Rashid, H., Vandergrift, W.A., Parashos, A., et al., 2024. Quantifying hubness to predict surgical outcomes in epilepsy: Assessing resection-hub alignment in interictal intracranial EEG networks. Epilepsia 65, 3362–3375. https://doi.org/10.1111/epi.18128.

van den Heuvel, M.P., Hulshoff Pol, H.E., 2010. Exploring the brain network: a review on resting-state fMRI functional connectivity. Eur. Neuropsychopharmacol. 20, 519–534. https://doi.org/10.1016/j.euroneuro.2010.03.008.

van den Heuvel, M.P., Sporns, O., 2013. Network hubs in the human brain. Trends Cogn. Sci. 17, 683–696. https://doi.org/10.1016/j.tics.2013.09.012.

Höller, Y., Helmstaedter, C., Lehnertz, K., 2018. Quantitative Pharmaco-Electroencephalography in Antiepileptic Drug Research. CNS Drugs 32, 839–848. https://doi.org/10.1007/s40263-018-0557-x.

Huang, Z.C., Shen, D.L., 1993. The prognostic significance of diazepam-induced EEG changes in epilepsy: a follow-up study. Clin. Electroencephalogr. 24, 179–187. https://doi.org/10.1177/155005949302400409.

Hughes, S.W., Crunelli, V., 2005. Thalamic mechanisms of EEG alpha rhythms and their pathological implications. Neuroscientist 11, 357–372. https://doi.org/10.1177/1073858405277450.

Iosifescu, D.V., 2011. Electroencephalography-derived biomarkers of antidepressant response. Harv. Rev. Psychiatry 19, 144–154. https://doi.org/10.3109/10673229.2011.586549.

Kanai, S., Oguri, M., Okanishi, T., Miyamoto, Y., Maeda, M., Yazaki, K., et al., 2024. Predictive modeling based on functional connectivity of interictal scalp EEG for infantile epileptic spasms syndrome. Clin. Neurophysiol. 167, 37–48. https://doi.org/10.1016/j.clinph.2024.08.016.

Lachaux, J.P., Rodriguez, E., Martinerie, J., Varela, F.J., 1999. Measuring phase synchrony in brain signals. Hum. Brain Mapp. 8, 194–208. https://doi.org/10.1002/(sici)1097-0193(1999)8:4.194::aid-hbm4>3.0.co;2-c.

Lanzone, J., Ricci, L., Tombini, M., Boscarino, M., Mecarelli, O., Pulitano, P., et al., 2021. The effect of Perampanel on EEG spectral power and connectivity in patients with focal epilepsy. Clin. Neurophysiol. 132, 2176–2183. https://doi.org/10.1016/j.clinph.2021.05.026.

Li, K.-Y., Huang, L.-C., Chang, Y.-P., Yang, Y.-H., 2020. The effects of lacosamide on cognitive function and psychiatric profiles in patients with epilepsy. Epilepsy Behav. 113, 107580. https://doi.org/10.1016/j.yebeh.2020.107580.

Lüttjohann, A., van Luijtelaar, G., 2022. The role of thalamic nuclei in genetic generalized epilepsies. Epilepsy Res. 182, 106918. https://doi.org/10.1016/j.eplepsyres.2022.106918.

Mucci, A., Volpe, U., Merlotti, E., Bucci, P., Galderisi, S., 2006. Pharmaco-EEG in psychiatry. Clin. EEG Neurosci. 37, 81–98. https://doi.org/10.1177/155005940603700206.

Pellegrino, G., Mecarelli, O., Pulitano, P., Tombini, M., Ricci, L., Lanzone, J., et al., 2018. Eslicarbazepine Acetate Modulates EEG Activity and Connectivity in Focal Epilepsy. Front. Neurol. 9, 1054. https://doi.org/10.3389/fneur.2018.01054.

Pellegrino, G., Tombini, M., Curcio, G., Campana, C., Di Pino, G., Assenza, G., et al., 2017. Slow Activity in Focal Epilepsy During Sleep and Wakefulness. Clin. EEG Neurosci. 48, 200–208. https://doi.org/10.1177/1550059416652055.

Ricci, L., Assenza, G., Pulitano, P., Simonelli, V., Vollero, L., Lanzone, J., et al., 2021. Measuring the effects of first antiepileptic medication in Temporal Lobe Epilepsy: Predictive value of quantitative-EEG analysis. Clin. Neurophysiol. 132, 25–35. https://doi.org/10.1016/j.clinph.2020.10.020.

Ricci, L., Croce, P., Pulitano, P., Boscarino, M., Zappasodi, F., Narducci, F., et al., 2022. Levetiracetam Modulates EEG Microstates in Temporal Lobe Epilepsy. Brain Topogr. 35, 680–691. https://doi.org/10.1007/s10548-022-00911-2.

Ricci, L., Tombini, M., Savastano, E., Pulitano, P., Piccioli, M., Forti, M., et al., 2024. Quantitative EEG analysis of brivaracetam in drug-resistant epilepsy: A pharmaco-EEG study. Clin. Neurophysiol. 163, 152–159. https://doi.org/10.1016/j.clinph.2024.04.023.

Ridley, B.G.Y., Rousseau, C., Wirsich, J., Le Troter, A., Soulier, E., Confort-Gouny, S., et al., 2015. Nodal approach reveals differential impact of lateralized focal epilepsies on hub reorganization. Neuroimage 118, 39–48. https://doi.org/10.1016/j.neuroimage.2015.05.096.

Rogawski, M.A., Löscher, W., 2004. The neurobiology of antiepileptic drugs. Nat. Rev. Neurosci. 5, 553–564. https://doi.org/10.1038/nrn1430.

Rubinov, M., Sporns, O., 2010. Complex network measures of brain connectivity: uses and interpretations. Neuroimage 52, 1059–1069. https://doi.org/10.1016/j.neuroimage.2009.10.003.

Saletu, B., Anderer, P., Kinsperger, K., Grünberger, J., 1987. Topographic brain mapping of EEG in neuropsychopharmacology–Part II. Clinical applications (pharmaco EEG imaging). Methods Find. Exp. Clin. Pharmacol. 9, 385–408.

Shi, X., Sundareswaran, R., Shanmugapriya, M., Jayaguptha, N., Khan, A., 2025. Graph based link prediction for epilepsy drug discovery. Sci. Rep. 15, 34087. https://doi.org/10.1038/s41598-025-14550-7.

Tadel, F., Baillet, S., Mosher, J.C., Pantazis, D., Leahy, R.M., 2011. Brainstorm: a user-friendly application for MEG/EEG analysis. Comput. Intell. Neurosci. 2011, 879716. https://doi.org/10.1155/2011/879716.

Tan, E., Troller-Renfree, S.V., Morales, S., Buzzell, G.A., McSweeney, M., Antúnez, M., et al., 2024. Theta activity and cognitive functioning: Integrating evidence from resting-state and task-related developmental electroencephalography (EEG) research. Dev. Cogn. Neurosci. 67, 101404. https://doi.org/10.1016/j.dcn.2024.101404.

Vecchio, F., Miraglia, F., Maria, R.P., 2017. Connectome: Graph theory application in functional brain network architecture. Clinical Neurophysiology Practice 2, 206–213. https://doi.org/10.1016/j.cnp.2017.09.003.

Vecchio, F., Miraglia, F., Marra, C., Quaranta, D., Vita, M.G., Bramanti, P., et al., 2014. Human brain networks in cognitive decline: a graph theoretical analysis of cortical connectivity from EEG data. J. Alzheimers Dis. 41, 113–127. https://doi.org/10.3233/JAD-132087.

Yang, C., Peng, Y., Zhang, L., Zhao, L., 2021. Safety and Tolerability of Lacosamide in Patients With Epilepsy: A Systematic Review and Meta-Analysis. Front. Pharmacol. 12, 694381. https://doi.org/10.3389/fphar.2021.694381.